

Kinetic and Isotherm Studies on Reactive Blue 21 Dye Adsorption from Aqueous Solutions by Cac

Sanaa El Aggadi, MariemEnnouhi, GhizlanKaichouh, Zoubida El Abbassi, Abderrahim El Hourch

Department of Chemistry, Faculty of Sciences, Mohammed V University in Rabat, Rabat, Morocco
sanaa_elaggadi@um5.ac.ma

ABSTRACT

This work is intended to investigate the possibility of using commercial activated carbon (CAC) as an adsorbent to remove the reactive blue 21 (RB21) dye from an aqueous solution by following the batch adsorption technique at room temperature ($25\pm1^{\circ}\text{C}$). The effect of adsorbent dosage, initial pH and contact time were studied. The results showed that increasing the CAC dosage from 0.5 to 5 g.L⁻¹ raised the RB21 adsorption rates from 92.16 % up to 99.99 %. The acidic condition (pH< 7) proved to be effective for RB21 adsorption studies. The adsorption process was fast, and it reached equilibrium in 2 hours of contact time. The kinetic parameters achieved at different concentrations were analyzed using a pseudo-first order, pseudo-second order and Elovich models. The experimental data fitted very well the pseudo-first order kinetic model. The experimental data were evaluated and fit well with the Freundlich and Temkin models. The study showed that CAC could be used as an efficient adsorbent material for the adsorption of RB21 dye from aqueous solution.

Keywords: Reactive blue 21, Activated carbon, Adsorption, CAC, Isotherm, Kinetics.

1 INTRODUCTION

The rapid expansion of modern industry has made water contamination a serious problem due to the uncontrolled emission of pollutants from factories(Liu, 2020). Dyes are one of the largest sources of these pollutants because of their pervasive applications in textiles, cosmetics, paper and many other industries(Saratale, 2020; S. El Aggadi, 2021). They present an important risk to aquatic life and the environment because they may block the penetration of sunlight from the water surface, thus preventing photosynthesis. Moreover, they raise the biochemical oxygen demand of the water, thus decreasing the reoxygenation process, which eventually inhibits the growth of photoautotrophic organic compounds (Mahlalela, 2016). On the other hand, most dyes are carcinogenic, toxic, teratogenic and take a long time to be photo/bio-degraded by the environment itself (Liu, 2019). Currently, there are many methods for treating dye wastewater, such as electrocoagulation(Núñez, 2019), electrochemical oxidation(Sanaa El Aggadi, 2021), ozonation (Wang, 2020), adsorption (Hassan, 2020), membrane separation(Zwane, 2018)and Photo-catalysis (Mahlalela, 2016; Ravichandran, 2020). Adsorption represents a successful and promising approach because of its ease of use, its low cost, the absence of secondary pollutants and the wide availability of adsorbent materials (Liu, 2019). Adsorption on activated carbon is widely employed because of its ability to separate a wide variety of chemical compounds, its effectiveness and its economic feasibility (Rahimian, 2020; Zhang, 2021).

Activated carbons are largely used as adsorbents in wastewater treatment due to their high surface areas, high adsorption capacities, rapid adsorption kinetics, micropore volumes and amphoteric properties, which allow the adsorption of both cationic and anionic pollutants in the effluent(Djilani, 2015; Han, 2020).

The present work reports the use of CAC for the adsorptive removal of RB21 dye from aqueous solution. Effects of such parameters as adsorbent dosage, initial pH, contact time and initial dye concentration on the adsorption process have been investigated by using the batch adsorption technique. Moreover, the study of adsorption kinetic and adsorption isothermal was also examined by various models to explore the adsorption mechanism.

2 MATERIALS AND METHODS

2.1 Materials

All experiments were carried out using CAC as adsorbent which was supplied by PICA CharbonActif. Reactive blue 21 dye ($C_{40}H_{25}CuN_9O_{14}S_5$) was purchased from Sigma-Aldrich. sulfuric acid and sodium hydroxide of analytical grade were purchased from Sigma-Aldrich. Chemicals used in this work were all reagent grade and were used with no further purification. Double deionized water was used for all solutions.

2.2 Adsorption experiments

The adsorption tests were conducted in the batch mode. For each experimental run, in a conical flask of 30 ml, a certain amount of CAC was added to 25 ml of dye solutions of known concentration. The effective factors such as pH (3-11), CAC dose ($0.5-5 \text{ g.L}^{-1}$), initial dye concentration ($0-200 \text{ mg.L}^{-1}$) and contact time (0-1440 min) were studied. The initial pH of the solution was adjusted with 0.1 M H_2SO_4 or 0.1 M NaOH solutions and determined with pH meter. The sample containing CAC was shaken to enhance adsorption efficiency (%). The suspension was filtered and the concentration of RB21 in the aqueous phase was determined using a UV-visible spectrophotometer (Analytik Jena, Specord 210 plus). The adsorption amount Q_e (mg.g^{-1}) and the dye removal efficiency E (%) of the sample were calculated using the following formulas(Feng, 2020):

$$Q_e = \frac{(C_0 - C_e) * V}{m} \quad (1)$$

$$E (\%) = \frac{(C_0 - C_e)}{C_0} * 100\% \quad (2)$$

Where C_0 and C_e are the initial and equilibrium dye concentration (mg.L^{-1}), respectively. V is the volume of solution (ml) and m is the mass of adsorbent (mg).

3 RESULTS AND DISCUSSION

3.1 Adsorption experiments

3.1.1 Effect of adsorbent dosage

The effect of adsorbent dosage on the removal efficiency of RB21 by CAC was validated by varying the adsorbent dose from 0.5 to 5 g.L^{-1} for the dye concentration of 200 mg.L^{-1} at natural pH, as shown in Figure 1. From the figure it can be observed that increasing the adsorbent dose increased the percent removal of RB21 from 92.16 % up to 99.99 %. This is

explained by the increase in adsorbent surface area and availability of more adsorption site of the adsorbent (Idan, 2017). Therefore, the quantity of dye adsorbs increases. Increasing of adsorbent dosage above 2 g.L⁻¹ had meager effect on the increase in removal efficiency of RB21. This may be imputed to the formation of aggregates at higher solid/liquid ratios or to sediment of particles (Fakhri, 2017).

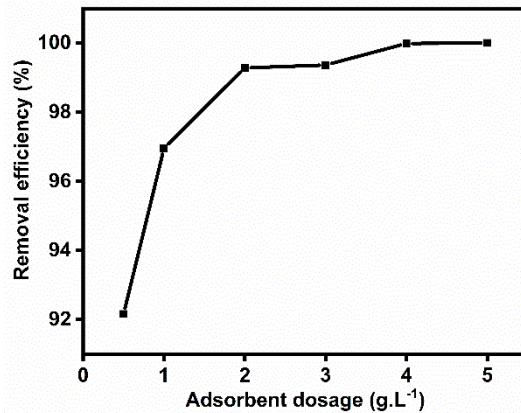


Figure 1: Effect of adsorbent dose on the removal efficiency of RB21 onto CAC, $C_0 = 100$ mg.L⁻¹, $t = 6$ h, $V = 25$ ml, $T = 25^\circ\text{C}$.

3.1.2 Effects of initial solution pH

To study the effect of initial pH on adsorption, experiments were carried out in the pH range 3–11 for RB21 removal (Figure 2). It can be seen that by increasing the pH value from 3 to 11, the removal of the RB21 by CAC is slightly reduced. Indeed, the rate of dye removal by adsorption is high and stable under acidic pH conditions and decreases slightly with increasing pH value under alkaline pH conditions. This trend can be explained by the fact that at low pH, dye molecules easily penetrate the pore structure of the CAC surface. A lower adsorption of the dye at alkaline pH is probably due to the presence of an excess of OH⁻ ions competing with RB21 for the hydrogen bond formed with the CAC coordinated water molecules in the interlayer (Fakhri, 2017).

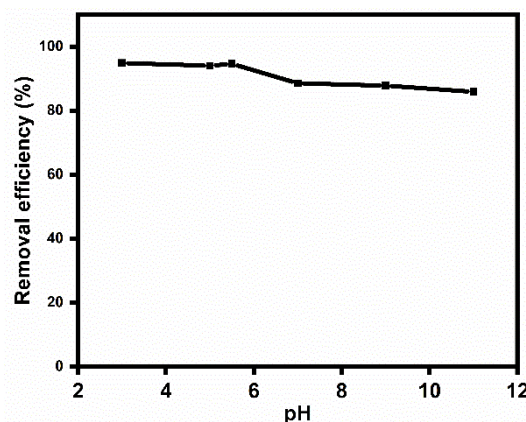


Figure 2: Effect of initial pH on the removal efficiency of RB21 onto CAC ($C_0 = 100$ mg.L⁻¹, $t = 2$ h, $V = 25$ ml, CAC dosage = 1 g.L⁻¹, $T = 25^\circ\text{C}$).

3.2 Adsorption kinetics studies

The effect of contact time on the adsorption capacity of RB21 dye for 24 hours using CAC at room temperature is shown in Figure 3. The uptake of RB21 dye increases sharply after 20 min have elapsed and reaches saturation after 120 min. The adsorption was faster at the beginning may be due to the availability of the uncovered surface area of the adsorbents (Aljeboree, 2017). However, over time, these active sites were occupied progressively by the dye molecules and a decrease in the adsorption sites of the remaining dye molecules in the solution was observed. Similar observations have been reported for the adsorption of dyes on other adsorbents, such as adsorption of reactive blue 19 onto lignocellulosic waste (Değermenci, 2019) and Congo red onto chitosan (Ma, 2019).

The kinetics of the adsorption process of RB21 on CAC were studied by fitting the experimental adsorption data determined at different contact times using the nonlinear forms of the pseudo-first order (Eq. (3)), pseudo-second order (Eq. (4)) and Elovich (Eq. (5)) models (Aljeboree, 2017; Falahian, 2018; Henning, 2019), as depicted in Figure 5.

$$Q_t = Q_e(1 - e^{-K_1 t}) \quad (3)$$

$$Q_t = \frac{K_2 Q_e^2 t}{1 + K_2 Q_e t} \quad (4)$$

$$Q_t = \frac{1}{\beta} \ln[\alpha \beta t + 1] \quad (5)$$

Where Q_e (mg.g^{-1}) and Q_t (mg.g^{-1}) are the adsorption capacities at equilibrium and at time t (min), respectively. K_1 (min^{-1}) and K_2 ($\text{g}.\text{mg}^{-1}.\text{min}^{-1}$) are the pseudo-first order rate constant and the pseudo-second order rate constant, respectively. α ($\text{mg.g}^{-1}.\text{min}^{-1}$) and β ($\text{g}.\text{mg}^{-1}$) are the initial adsorption rate constant and the desorption rate, respectively.

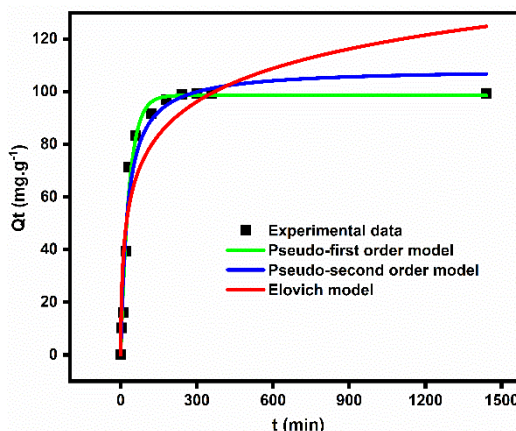


Figure 3: Nonlinear fitting of kinetic models for the adsorption of RB21 dye on CAC adsorbent ($C_0 = 100 \text{ mg.L}^{-1}$, $T = 25^\circ\text{C}$, $V = 25 \text{ ml}$, CAC dosage = 1 g.L^{-1}).

The nonlinear fitting results of the kinetic model are shown in Figure 3 and Table 1. The correlation coefficient ($R^2 = 0.98$) of the pseudo-first order kinetic equation was higher than that of the pseudo-second order kinetic equation ($R^2 = 0.96$), and the theoretical adsorption capacity $Q_e(\text{cal})$ of the pseudo-first order kinetic model was closer to the experimental measured value $Q_e(\text{exp})$, we can say that the pseudo-first order fits best than the pseudo-second order kinetics. The correlation coefficients (R^2) of Elovich model ($R^2 = 0.87$) was not high enough to describe the RB21 adsorption process.

Table 1: Parameters for pseudo-first order, pseudo-second order and Elovich kinetic models

for RB21 adsorption.

Models	Parameter	Value
Pseudo-first order	Q_e (exp) (mg.g ⁻¹)	99.46
	Q_e (cal) (mg.g ⁻¹)	98.62
	K_1 (min ⁻¹)	0.03
	R^2	0.98
Pseudo-second order	Q_e (exp) (mg.g ⁻¹)	99.46
	Q_e (cal) (mg.g ⁻¹)	108.76
	K_2 (g.mg ⁻¹ .min ⁻¹)	0.000347
	R^2	0.96
Elovich	α (mg g ⁻¹ min ⁻¹)	11.67
	β (g mg ⁻¹)	0.05
	R^2	0.87

3.3 Adsorption isotherm

Adsorption equilibrium data expressing the relationship between the mass of adsorbate adsorbed per unit weight of adsorbent and the equilibrium liquid phase concentration of the adsorbate are plotted by adsorption isotherms and provide important design data for the adsorption system. In this study, the non-linear forms of the Langmuir, Freundlich and Temkin isotherm models were used to analyze the RB21 removal equilibrium data. Comparisons of linear and nonlinear regressions often concluded that the best parameter estimates were returned by nonlinear optimizations (Allen, 2003; Ho, 2004; Boulinguez, 2008).

3.3.1 Langmuir isotherm

The Langmuir adsorption isotherm (Langmuir, 1916) assumes that the adsorption sites are monolayer, uniform and finite, so that a saturation value is reached beyond which no additional adsorption takes place. It also assumes that there is no interaction between the molecules adsorbed on neighboring sites. The Langmuir equation which is valid for monolayer adsorption onto a surface with a finite number of identical sites is given by Eq. (6):

$$Q_e = \frac{Q_m K_L C_e}{1 + K_L C_e} \quad (6)$$

Where Q_e (mg.g⁻¹) is the adsorption capacity of the adsorbent at equilibrium, Q_m (mg.g⁻¹) is the maximum adsorption capacity, C_e (mg.L⁻¹), is the concentration of the dye solution at equilibrium and K_L (L.mg⁻¹) is the Langmuir equilibrium adsorption constant related to energy of adsorption which quantitatively reflects the affinity between the adsorbent and adsorbate.

3.3.2 Freundlich isotherm

The Freundlich isotherm (Freundlich, 1906) is an empirical equation for multilayer, heterogeneous adsorption sites. The Freundlich equation is commonly given by Eq. (7):

$$Q_e = K_F C_e^{1/n} \quad (7)$$

K_F (L.g⁻¹) is the Freundlich constant related to adsorption capacity and $1/n$ is the intensity of

the adsorption or surface heterogeneity indicating the relative distribution of the energy and the heterogeneity of the adsorbate sites.

3.3.3 Temkin isotherm

Based on Temkin isotherm (Temkin, 1940) the adsorbent surface is heterogeneous, binding energy is distributed uniformly and heat of adsorption decreases linearly with adsorption quantity. The nonlinear form of Temkin isotherm express as Eq. (8) as follows:

$$Qe = \left(\frac{RT}{b} \right) \ln \left(\frac{K_T}{R} Ce \right) \quad (8)$$

Where; K_T is the equilibrium binding constant (L.g^{-1}), b is Temkin constant related to heat of adsorption (J.mol^{-1}), R is the universal gas constant ($8.314 \text{ J.mol}^{-1} \text{ K}^{-1}$) and T is the absolute temperature (K).

Fitted models parameters from nonlinear regressive method are listed in Table 2. A comparison of nonlinear fitted curves from experimental data and three different isotherms is shown in Figure 4. On the basis of the R^2 values, the experimental data were best fitted by the Freundlich ($R^2 = 0.91$) and Temkin ($R^2 = 0.92$) isotherm models than the Langmuir ($R^2 = 0.6$) isotherm, indicating adsorption onto heterogeneous CAC surface. Generally speaking, adsorption was difficult when $1/n < 2$, linear when $n=1$, and was easy when $0.1 < 1/n < 0.5$ (Hu, 2021). The value of $1/n$ in the experiment was less than 0.5, which indicated that the surface of the adsorbent is heterogenous in nature (Aroguz, 2006). In addition, Temkin isotherm shows a strong affinity for the adsorption capacity of RB21 on CAC. An indication of the decrease in heat of adsorption as the dye coverage of the CAC surface increases is the fact that adsorption follows the Temkin isotherm (Koçer, 2016). A similar results were reported in literature for the adsorption of turquoise blue QG reactive dye from aqueous solution by commercial activated carbon (Schimmel, 2010), and adsorption of methyl red on activated carbon derived from custard apple (Khan, 2018).

Table 2: The fitting parameters of adsorption isotherms for RB21 adsorption by CAC.

Isotherm	Parameter	Value
Langmuir	$Q_m (\text{mg.g}^{-1})$	147.5
	$K_L (\text{L.mg}^{-1})$	2.27
	R^2	0.6
Freundlich	$K_F (\text{mg.g}^{-1})$	102.03
	$1/n$	0.106
	R^2	0.91
Temkin	$K_T (\text{L.g}^{-1})$	165177.86
	$b (\text{J.mol}^{-1})$	265.5
	R^2	0.92

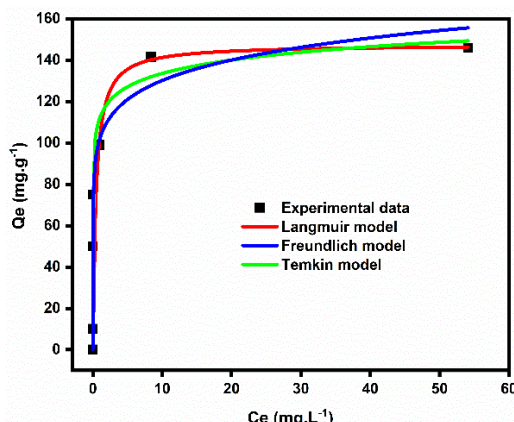


Figure 4: Nonlinear fitting of adsorption isotherms of RB21 dye on CAC adsorbent ($C_0 = 100 \text{ mg.L}^{-1}$, $T = 25 \text{ }^{\circ}\text{C}$, $V = 25 \text{ ml}$, CAC dosage = 1 g.L^{-1}).

4 CONCLUSIONS

The adsorption behavior of RB21 from aqueous solution onto CAC was investigated in the batch mode demonstrate that the adsorption is affected by various conditions such as adsorbent dosage, initial pH and contact time. The kinetic studies revealed that pseudo-firstorder kinetic is best suited to explain the adsorption process. The adsorption process followed the Freundlich and Temkin isothermal models with significant correlation coefficients ($R^2 > 0.91$). Therefore, we conclude that CAC material can be used as highly efficient adsorbent and for the removal of phthalocyanine dyes from wastewater, in particular the dye RB21 dye.

REFERENCES

1. El Aggadi, Sanaa *et al.*, 2021. *E3S Web of Conferences*, 234.
2. El Aggadi, S., El Abbassi, Z. and El Hourch, A., 2021. *Desalination and Water Treatment*, 215.
3. Aljeboree, A. M., Alshirifi, A. N. and Alkaim, A. F., 2017. *Arabian Journal of Chemistry*, 10.
4. Allen, S. J. *et al.*, 2003. *Bioresource Technology*, 88(2).
5. Aroguz, A. Z., 2006. *Journal of Hazardous Materials*, 135(1–3).
6. Boulinguez, B., Le Cloirec, P. and Wolbert, D., 2008. *Langmuir*, 24(13).
7. Değermenci, G. D. *et al.*, 2019. *Journal of Cleaner Production*, 225.
8. Djilani, C. *et al.*, 2015. *Journal of the Taiwan Institute of Chemical Engineers*, 53.
9. Fakhri, A., 2017. *Journal of Saudi Chemical Society*, 21.
10. Falahian, Z., Torki, F. and Faghihian, H., 2018. *Global Challenges*, 2(1).
11. Feng, C. *et al.*, 2020. *New Journal of Chemistry*, 44(6).
12. Freundlich, H. M., 1906. *Journal of Physicochemical*, 57A(1).
13. Han, Q. *et al.*, 2020. *Powder Technology*, 366.
14. Hassan, W. *et al.*, 2020. *Surfaces and Interfaces*, 20.
15. Henning, L. M. *et al.*, 2019. *RSC Advances*, 9(62).
16. Ho, Y. S., 2004. *Carbon*. Elsevier Ltd.
17. Hu, Y. ying *et al.*, 2021. *Journal of Hazardous Materials*, 401.

18. Idan, I. J., 2017. *OALib*, 04(07).
19. Khan, E. A., Shahjahan and Khan, T. A., 2018. *Journal of Molecular Liquids*, 249.
20. Koçer, O. and Acemioğlu, B., 2016. *Desalination and Water Treatment*, 57(35).
21. Langmuir, I., 1916. *Journal of the American Chemical Society*, 38(11).
22. Liu, J., Yu, H. and Wang, L., 2020. *Journal of Hazardous Materials*, 392.
23. Liu, X. *et al.*, 2019. *Journal of Hazardous Materials*, 373.
24. Ma, H. *et al.*, 2019. *Journal of Cleaner Production*, 214.
25. Mahlalela, L. C. and Dlamini, L. N., 2016. *Surfaces and Interfaces*, 1–3.
26. Núñez, J. *et al.*, 2019. *Journal of Hazardous Materials*, 371.
27. Rahimian, R. and Zarinabadi, S., 2020. *Progress in Chemical and Biochemical Research*, 3(3).
28. Ravichandran, K., Dhanraj, C. and Kavitha, P., 2020. *Surfaces and Interfaces*, 20.
29. Saratale, R. G. *et al.*, 2020. in *Bioremediation of Industrial Waste for Environmental Safety*. Springer Singapore.
30. Schimmel, D. *et al.*, 2010. *Brazilian Journal of Chemical Engineering*, 27(2).
31. Temkin, M. I., 1940. *Acta physiochim. URSS*, 12.
32. Wang, J. and Chen, H., 2020. *Science of the Total Environment*. Elsevier B.V.
33. Zhang, Z. *et al.*, 2021. *Microporous and Mesoporous Materials*, 315.
34. Zwane, S. *et al.*, 2018. *Surfaces and Interfaces*, 13.